Sustainability in Mechanical and Materials Design

smmd.pol-aca.com

Article

Research on Failure Behavior of Metal Matrix Composites Based on Phase Field Method and Cohesive Zone Model

Yao Dong [1],Xi Chen[2] ,Haodong Yang [3*]

[1]Guizhou Qiannan College of Economic ,School of Computer Engineering, Qiannan, Guizhou, United Kingdom.
[2]Quanzhou University of Information Engineering, School of Mechanical Engineering,Quanzhou, Fujian, China.
[3]Kaili University, School of Mechanical Engineering, Kaili,Guizhou, China.

ARTICLE INFO

Keywords:
Metal matrix composites
Phase field method
Cohesive zone model
Thermo-mechanical coupling
Rate-dependent damage
Failure mechanism

ABSTRACT

The failure mechanisms of metal matrix composites (MMCs) under extreme environments such as high temperature and high strain rates are key issues restricting their reliable application. This paper develops a thermo-mechanical-rate coupled phase field-cohesive zone model to simulate the synergistic failure behavior of their matrix and interface. By introducing a temperature degree of freedom and rate-dependent functions, the model achieves dynamic evolution of cohesive strength and fracture energy with temperature and strain rate. The results show that the rate parameters ζ_1 and ζ_2 significantly affect the cohesive strength and failure displacement, respectively, while the temperature parameters κ_T and ς_T dominate the thermal softening effect and fracture energy degradation. Obvious competition among failure modes is observed under different working conditions: high strain rates promote increased cohesive strength and particle fracture, while high temperatures lead to strength softening and interface debonding dominance. This model provides an effective analysis tool and theoretical basis for revealing the damage mechanisms of multiphase materials under thermo-mechanical coupled loads.

1. Introduction

Metal Matrix Composites (MMCs) are widely used in high-end equipment fields such as aerospace, shipbuilding, and wind power generation due to their high specific strength, good corrosion resistance, and excellent high-temperature performance [1]. However, due to their multiphase heterogeneous microstructure, MMCs often exhibit various failure modes during service, such as matrix cracking, reinforcement fracture, and interface debonding. These modes are often coupled, significantly increasing the complexity of mechanical behavior prediction [2]. Traditional single failure models struggle to comprehensively capture their damage evolution mechanisms. Therefore, developing numerical models that

* **Correspondence authors**

Email address:2430839554@qq.com

Citation: To be added by editorial staff during production.

couple multiple physical fields and synergize multiple failure mechanisms is of great significance for enhancing the reliability design and life prediction capabilities of MMCs.

In recent years, the combination of the Phase Field Method (PFM) and the Cohesive Zone Model (CZM) has proven effective in simulating the entire process from microscopic damage initiation to macroscopic crack propagation [3]. However, most existing models are limited to room temperature and quasi-static conditions, seldom considering the widespread strain rate effects and temperature influences present in actual working conditions. Therefore, this paper aims to establish a thermo-mechanically coupled rate-dependent damage model, combining the ductile phase field method with cohesive elements, to systematically study the multi-mode failure behavior of metal matrix composites under complex loads.

2. Literature Review

Research on failure modeling of Metal Matrix Composites (MMCs) has gradually evolved from early macroscopic phenomenological models to modern numerical methods based on microscopic physical mechanisms. Despite significant progress, accurately capturing multiphase interface behavior, thermo-mechanical-rate coupling effects, and the competition mechanisms among various failure modes remains a challenge and focus of current research.

In early studies, Continuum Damage Mechanics (CDM) was widely used to simulate the progressive failure process of composites. For instance, Ladevèze et al. [4] proposed an energy dissipation-based CDM model that effectively predicted matrix cracking and fiber fracture in laminated composites. However, such models often lack explicit interface characterization capabilities, making it difficult to accurately capture interface debonding behavior. To address this, the eXtended Finite Element Method (XFEM) was introduced to simulate discontinuous interfaces. The work of Belytschko et al. [5] showed that XFEM could simulate crack growth without remeshing, but it still faces challenges in handling multiple crack interactions and complex interface topologies.

To specifically address interface problems, the Cohesive Zone Model (CZM) has been widely used since Needleman's pioneering work [6]. Traditional CZMs use traction-separation laws to describe interface damage, but most are limited to room temperature and quasi-static conditions. In actual working conditions, strain rate effects significantly influence interface mechanical behavior. In this regard, Rahul et al. [7] developed a rate-dependent CZM. By introducing a strain rate sensitivity factor, they successfully predicted the interface debonding process of composites under high strain rates. However, this model did not consider the influence of temperature variation, limiting its application under thermomechanical loading conditions.

Regarding thermo-mechanical coupling modeling, Rousseau et al. [8] made significant contributions. They proposed a temperature-dependent cohesive law, describing the weakening effect of temperature on interface strength by introducing a thermal softening coefficient. Specifically, their study showed that the interface strength of SiC/Ti composites decreased by 15-20% in the range of 200°C to 400°C. Similarly, Lin et al. [9], by considering residual stresses caused by thermal expansion mismatch, found that thermal cycling

loads significantly accelerate the accumulation of interface damage. However, these models mostly focus on the interface behavior itself and fail to effectively couple with the damage evolution of the matrix.

On the other hand, the Phase Field Method (PFM) has recently shown unique advantages in simulating complex crack paths. The phase field fracture model established by Miehe et al. [10] can naturally describe crack initiation, branching, and merging without(pre-defining) the crack path. Borden et al. [11] further extended it to dynamic fracture problems, successfully simulating crack propagation patterns under impact loads. However, the standard phase field method has shortcomings in handling material interfaces, especially when the interface strength differs significantly from the matrix properties.

Recently, researchers have begun exploring the combination of PFM and CZM to leverage their respective advantages. Teichtmeister et al. [12] first achieved the coupling of the phase field method and the cohesive zone model, enabling simultaneous simulation of matrix cracking and interface debonding. Guo et al. [13] further developed a phase field-cohesive model considering ductile damage and verified its effectiveness through comparison with experiments. However, most of these studies are still limited to isothermal conditions and fail to fully consider the thermo-mechanical-rate multi-field coupling effects present in actual service environments.

It is noteworthy that under high temperature and high strain rate conditions, material interface behavior exhibits complex competition mechanisms. On one hand, increasing temperature leads to decreased interface strength (thermal softening effect); on the other hand, increasing strain rate causes increased strength (strain rate hardening effect). Accurately describing this coupling effect remains a gap in current research. Furthermore, most existing models are insufficient in describing the interactions among multiple particle reinforcements, especially when considering randomly distributed and morphologically diverse reinforcements.

In summary, although existing research has made significant progress in MMC failure modeling, the following limitations remain: (1) Lack of a unified framework to simultaneously describe the thermal-rate dependent failure of the matrix and interface; (2) Most models fail to fully consider the influence of temperature on fracture energy; (3) The interaction mechanisms between multiple particle reinforcements and their impact on failure paths are still unclear; (4) Model parameters lack systematic experimental calibration, especially under extreme environmental conditions. This work aims to address these shortcomings by establishing a numerical model that comprehensively describes the failure behavior of metal matrix composites under multi-field coupled conditions.

3. Research Methods

3.1 Thermo-Mechanically Coupled Cohesive Zone Model

A cohesive element has eight nodes, each with three degrees of freedom corresponding to the normal and two tangential displacements. $\mathbf{u} = [u_{\mathrm{n}}^{i}, u_{\mathrm{t}}^{i}, u_{\mathrm{s}}^{i}]$,where $\boldsymbol{i}$ = 1, 2 ,…, 8, $\boldsymbol{i}$ represents the node number. To establish a thermo-mechanically coupled CZM, an additional degree of freedom is introduced to describe the

temperature effect， meaning each node has four degrees of freedom $\mathbf{u}=[u_{\mathrm{n}}^{i},u_{\mathrm{t}}^{i},u_{\mathrm{s}}^{i},T^{i}]$ ， where **T** is temperature. Compared to previous CZMs, this study introduces a temperature degree of freedom based on the traditional eight-node cohesive element, establishing an element form with four degrees of freedom (three displacements, one temperature). Global and local displacements are transformed using an extended rotation matrix R.

First, the relationship between global node displacements and local node displacements satisfies:

$$\bar{\mathbf{u}}=\mathbf{R}\hat{\mathbf{u}} \tag{3-1}$$

The rotation matrix R is modified to:

$$\mathbf{R}=\begin{bmatrix} \mathrm{n}^1 & \mathrm{n}^2 & \mathrm{n}^3 & 0 \\ \mathrm{t}^1 & \mathrm{t}^2 & \mathrm{t}^3 & 0 \\ \mathrm{s}^1 & \mathrm{s}^2 & \mathrm{s}^3 & 0 \\ 0 & 0 & 0 & 1 \end{bmatrix} \tag{3-2}$$

The opening displacement can be obtained from the local node displacements, with the relationship:

$$\bar{\boldsymbol{\Delta}}=\mathbf{L}\bar{\mathbf{u}} \tag{3-3}$$

Where， $\bar{\boldsymbol{\Delta}}$ is the nodal opening displacement vector， and $\mathbf{L}=[-\mathbf{I}_{16\times16}\quad \mathbf{I}_{16\times16}]$is the local displacement-separation matrix.Thus, the global opening displacement **Δ**of the cohesive element can be written as:

$$\boldsymbol{\Delta}=\mathbf{NLR}\hat{\mathbf{u}} \tag{3-4}$$

Based on the above equations, the force vector of the cohesive element can still be written as:

$$\mathbf{F}_{\mathrm{elem}}=\int_0^1\int_0^1\mathbf{B}^{\mathrm{T}}\mathbf{R}^{\mathrm{T}}\mathbf{t}_{\mathrm{local}}J\mathrm{d}\xi\mathrm{d}\eta \tag{3-5}$$

Where **B = NL**, and the superscript T denotes the transpose operation. Considering the free energy per unit area $\Psi(\Delta, d)$ can be expressed as follows :

$$\Psi(\Delta,d)=\frac{1}{2}(1-d_j)K_j\Delta_j^2\exp\left(-\kappa_T\frac{T-T_{\mathrm{ref}}}{T_{\mathrm{ref}}}\right) \tag{3-6}$$

Where κ_T is a temperature-dependent coefficient. The cohesive traction can be determined from the above equation:

$$\bar{t}_j=\frac{\partial\Psi(\Delta,d)}{\partial\Delta}=(1-d_j)K_j\Delta_j\exp\left(-\kappa_T\frac{T-T_{\mathrm{ref}}}{T_{\mathrm{ref}}}\right) \tag{3-7}$$

Equation (3-7) shows the influence of temperature on the cohesive traction. When $T = T_{\mathrm{ref}}$, this equation reduces to the traditional bilinear CZM. Furthermore, considering heat transfer in the cohesive zone, the heat flux per unit area is:

$$q_{\mathrm{ce}}=h_{\mathrm{ce}}\Delta T \tag{3-8}$$

Where q_{ce} is the heat flux per unit area crossing the cohesive element, and $\Delta T=T^{+}-T^{-}$ is the temperature difference between the upper and lower surfaces of the cohesive element. h_{ce} is the thermal conductivity of

the cohesive element, composed of the bond conductivity $h_{\mathrm{ce}}^{\mathrm{bond}}$, the surface contact conductivity $h_{\mathrm{ce}}^{\mathrm{contact}}$, and the air conductivity $h_{\mathrm{ce}}^{\mathrm{air}}$, expressed as follows :

$$h_{\mathrm{ce}} = h_{\mathrm{ce}}^{\mathrm{bond}} + h_{\mathrm{ce}}^{\mathrm{contact}} + h_{\mathrm{ce}}^{\mathrm{air}} = (1-d_j)h_{\mathrm{ce}}^{\mathrm{bond}} + d_j\left(h_{\mathrm{ce}}^{\mathrm{air}} \frac{\langle \Delta_{\mathrm{n}} \rangle}{\Delta_{\mathrm{n}}} + h_{\mathrm{ce}}^{\mathrm{contact}} \langle -\Delta_{\mathrm{n}} \rangle \right) \tag{3-9}$$

Note in Equation (3-9) that the contact conductivity and air conductivity only come into effect when the cohesive element is damaged. Additionally, when the cohesive element is under tension, the damaged surfaces are not in contact, so the contact conductivity does not appear; when under shear loading, the air conductivity is not considered; the air conductivity $h_{\mathrm{ce}}^{\mathrm{air}}$ is generally taken as 2.0 W/(mm²·K).

When materials are loaded under force in high-temperature environments, their stress decreases with increasing temperature, and the failure strain/displacement also changes with temperature [14, 15]. Therefore, to more accurately characterize the mechanical response of materials, besides considering the influence of temperature on stress, it is also necessary to consider the influence of temperature on failure strain/displacement. This analysis helps to more comprehensively understand the failure behavior of materials under high-temperature conditions.

3.2 Rate- and Temperature-Dependent Cohesive Zone Model

Based on previous CZMs, it is further extended to include strain rate and temperature effects. First, from Equation (3-7), it is known that when damage initiation occurs, the cohesive traction equals the cohesive strength $\overline{t}_j^{\,0}$, which can be written as:

$$\overline{t}_j^{\,0} = (1-d_j)K_j\Delta_j^0 \exp\left(-\kappa_T \frac{T-T_{\mathrm{ref}}}{T_{\mathrm{ref}}} \right) \tag{3-10}$$

Note that this equation explicitly describes the influence of temperature on cohesive strength. Related research [16, 17] indicates that the fracture toughness of metallic materials decreases with increasing temperature. Therefore, the rate- and temperature-dependent cohesive strength and critical fracture energy can be further modified as:

$$\overline{t}_j^{\,0}(\dot{\varepsilon}^{\mathrm{ce}}, T) = \begin{cases} (1-d_j)K_j\Delta_j^0 \exp\left(-\kappa_T \dfrac{T-T_{\mathrm{ref}}}{T_{\mathrm{ref}}} \right) & \dot{\varepsilon}^{\mathrm{ce}} \le \dot{\varepsilon}_{\mathrm{ref}} \\ (1-d_j)K_j\Delta_j^0 \exp\left(-\kappa_T \dfrac{T-T_{\mathrm{ref}}}{T_{\mathrm{ref}}} \right)\left[1 + f_1(\dot{\varepsilon}^{\mathrm{ce}}) \right] & \dot{\varepsilon}^{\mathrm{ce}} > \dot{\varepsilon}_{\mathrm{ref}} \end{cases} \tag{3-11}$$

$$G_{\mathrm{c}}(\dot{\varepsilon}^{\mathrm{ce}}, T) = \begin{cases} \left(G_{\mathrm{c}}\right)_{\mathrm{ref}} \exp\left(-\varsigma_T \dfrac{T-T_{\mathrm{ref}}}{T_{\mathrm{ref}}} \right) & \dot{\varepsilon}^{\mathrm{ce}} \le \dot{\varepsilon}_{\mathrm{ref}} \\ \left(G_{\mathrm{c}}\right)_{\mathrm{ref}} \exp\left(-\varsigma_T \dfrac{T-T_{\mathrm{ref}}}{T_{\mathrm{ref}}} \right)\left[1 + f_2(\dot{\varepsilon}^{\mathrm{ce}}) \right] & \dot{\varepsilon}^{\mathrm{ce}} > \dot{\varepsilon}_{\mathrm{ref}} \end{cases} \tag{3-12}$$

Where ς_T is a temperature-dependent coefficient. For convenience, this chapter takes $f_1(\dot{\varepsilon}^{ce})$ and $f_2(\dot{\varepsilon}^{ce})$ as two simple linear functions, rewritten as:

$$\overline{t}_j^0(\dot{\varepsilon}^{ce},T)=\begin{cases}(1-d_j)K_j\Delta_j^0\exp\left(-\kappa_T\dfrac{T-T_{ref}}{T_{ref}}\right) & \dot{\varepsilon}^{ce}\le\dot{\varepsilon}_{ref}\\ (1-d_j)K_j\Delta_j^0\exp\left(-\kappa_T\dfrac{T-T_{ref}}{T_{ref}}\right)\left[1+\zeta_1\ln\left(\dfrac{\dot{\varepsilon}^{ce}}{\dot{\varepsilon}_{ref}}\right)\right] & \dot{\varepsilon}^{ce}>\dot{\varepsilon}_{ref}\end{cases} \tag{3-13}$$

$$G_c(\dot{\varepsilon}^{ce},T)=\begin{cases}(G_c)_{ref}\exp\left(-\varsigma_T\dfrac{T-T_{ref}}{T_{ref}}\right) & \dot{\varepsilon}^{ce}\le\dot{\varepsilon}_{ref}\\ (G_c)_{ref}\exp\left(-\varsigma_T\dfrac{T-T_{ref}}{T_{ref}}\right)\left[1+\zeta_2\ln\left(\dfrac{\dot{\varepsilon}^{ce}}{\dot{\varepsilon}_{ref}}\right)\right] & \dot{\varepsilon}^{ce}>\dot{\varepsilon}_{ref}\end{cases} \tag{3-14}$$

4. Research Results

The reference strain rate $\dot{\varepsilon}_{ref}$ in this paper is selected as 1.0 s^{-1}. Next, the rate- and temperature-dependent CZM is implemented in ABAQUS/Explicit, and its characteristics are briefly illustrated through an element test. First, a three-dimensional cohesive element is still used and subjected to a tensile test to explore the influence of cohesive model parameters. In this example, it is assumed that the fracture energy, cohesive strength, and cohesive stiffness are the same in the normal and tangential directions. The material properties of the cohesive element are listed in Table 4-1 [14, 15], and the numerical simulation results are shown in Figure 4-1.

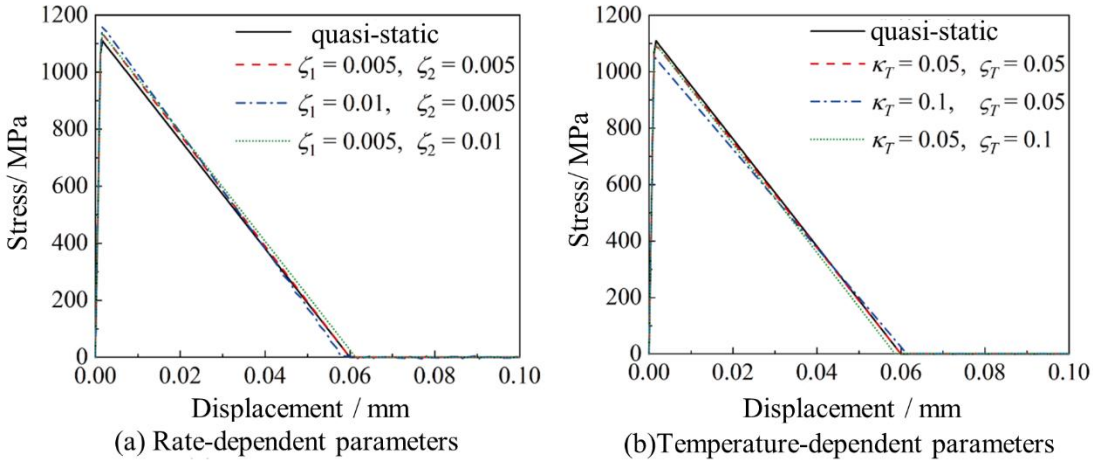

Figure 4-1 The impact of parameters on unit testing

From Figure 4-1(a), it can be seen that changes in the parameter ζ_1 affect the magnitude of the cohesive strength; the larger its value, the greater the cohesive strength. Conversely, the larger the value of ζ_2, the larger the failure displacement. In Figure 4-1(b), as the value of κ_T increases, the cohesive strength gradually decreases, meaning the thermal softening effect of temperature on cohesive strength becomes more pronounced. A larger value of ς_T results in a smaller failure displacement, indirectly reflecting the influence of temperature on fracture energy. In summary, the strain rate and temperature-dependent parameters determine the degree of strengthening or softening of the cohesive strength and fracture energy.

Table 4-1 Material properties of the cohesive element[14, 15]

Continuum Element		Cohesive Element	
Elastic Modulus E=/ GPa	109	Density ρ/ kg·m^{-3}	4430
Poisson's Ratio v	0.34	Fracture Energy$(G_{nc,tc,sc})_{ref}$ / N·mm^{-1}	30
Density ρ/ kg·m^{-3}	4430	Cohesive Strength $\overline{t}^{0}_{n,t,s}$ /MPa	1000
Specific Heat c_T/ J·(kg·K)$^{-1}$	611	Cohesive Stiffness $K_{n,s,t}$/N·mm^{-3}	1×10^{6}
Thermal Conductivity k_c / W·(m·K)$^{-1}$	6.8	Bond Conductivity h_{bond} / W·(m·K)$^{-1}$	45
		Contact Conductivity $h_{contact}$ / W·(m·K)$^{-1}$	100
		Air Conductivity h_{air} / W·(m·K)$^{-1}$	2

Additionally, taking the rate and temperature-dependent parameters ζ_1= 0.01, ζ_2= 0.005,κ_T = 0.05, ς_T= 0.1 as an example, the strain rate and temperature effect characteristics of the proposed model are elucidated. The numerical results are shown in Figure 4-2.

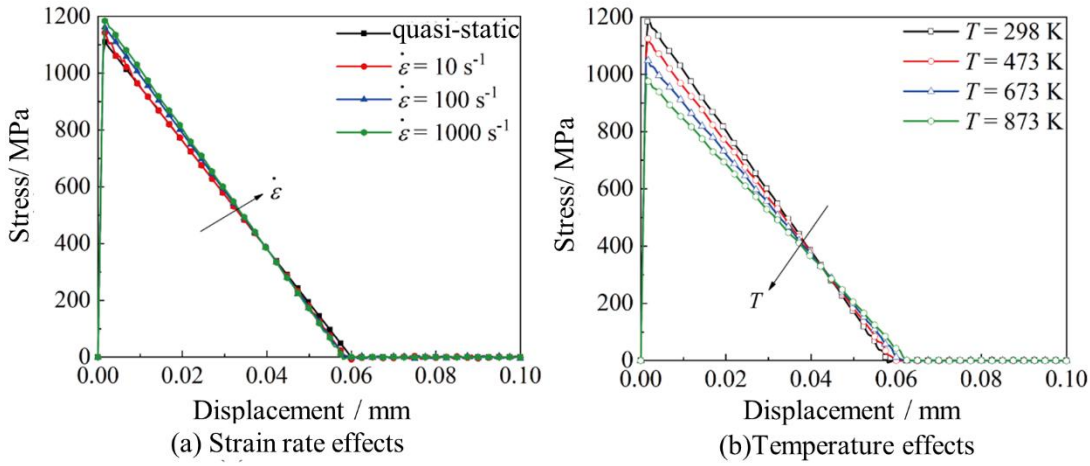

Figure 4-2 Thermo-mechanically coupled cohesive law

From Figure 4-2(a), it can be seen that as the strain rate increases, the cohesive strength also increases, but the change in failure displacement is small. This result means that under these circumstances, the influence of strain rate on fracture energy is minimal. However, in Figure 4-2(b), an increase in temperature leads to a gradual decrease in cohesive strength and an increase in failure displacement, showing the significant influence of temperature on both cohesive strength and fracture energy. Note that Figure 4-2(b) shows numerical results at a strain rate of 1000 s^{-1}. Overall, the current model can effectively characterize interface failure behavior under different strain rate and temperature conditions. Figure 4-2(b) indicates that temperature increase leads to decreased cohesive strength and increased failure displacement, suggesting

that higher temperatures promote the early initiation and propagation of interface damage. This result is consistent with the experimental phenomena reported in references [16, 17].

5. Summary and Outlook

This paper systematically studied the failure behavior of metal matrix composites under multi-field loads by establishing a thermo-mechanical-rate coupled phase field-cohesive zone model. The model successfully characterized the coupled effects of strain rate and temperature on cohesive strength and fracture energy, revealing the cross-scale failure mechanism from microscopic damage initiation to macroscopic crack propagation. The research results indicate that particle fracture dominates failure under high strain rates, while high temperature significantly promotes interface debonding. The thermo-mechanical coupling effect induces complex mixed-mode failure. This model provides an effective numerical tool for understanding and predicting the failure behavior of composite materials in extreme environments.

However, the current model parameters still rely on values from the literature, lacking direct experimental calibration for high-temperature and high-strain-rate interface behavior, and also not considering thermomechanical fatigue processes. The next steps will involve conducting dynamic thermomechanical experiments combined with in-situ observations to calibrate key model parameters; developing a fatigue damage submodel incorporating cyclic loading; and simultaneously combining multi-scale computation and machine learning methods to achieve a full-chain design from microstructure optimization to component performance prediction, significantly enhancing the service reliability of composite materials in aerospace engines and high thermal load structures.

Acknowledgments

This work has not received any funding support.

Conflicts of Interest

The authors declare that they have no known competing financial interests or personal relationships that could have appeared to influence the work reported in this paper.

References

[1] Chawla, K. K., et al. (2013). Materials Science and Engineering: R: Reports, 76(1), 1-46.

[2] LLorca, J., et al. (2011). Progress in Materials Science, 56(7), 711-809.

[3] Miehe, C., et al. (2010). Computer Methods in Applied Mechanics and Engineering, 199(45-48), 2765-2778.

[4] Ladevèze, P., Lubineau, G., & Marsal, D. (2006). Towards a bridge between the micro- and mesomechanics of delamination for laminated composites. Composites Science and Technology, 66(6), 698-712.

[5] Belytschko, T., & Black, T. (1999). Elastic crack growth in finite elements with minimal remeshing. International Journal for Numerical Methods in Engineering, 45(5), 601-620.

[6] Needleman, A. (1987). A continuum model for void nucleation by inclusion debonding. Journal of Applied Mechanics, 54(3), 525-531.

[7] Rahul, K., & Singh, I. V. (2018). A rate-dependent cohesive zone model for simulating high-speed crack growth. Engineering Fracture Mechanics, 189, 239-253.
[8] Rousseau, C. E., & Tippur, H. V. (2001). Evaluation of crack-tip fields and stress intensity factors in functionally graded materials with cracks along the elastic gradient. International Journal of Solids and Structures, 38(42-43), 7609-7627.
[9] Lin, G., & Cornec, A. (2000). A cohesive zone model for fatigue crack growth in quasibrittle materials. International Journal of Solids and Structures, 37(46-47), 6769-6790.
[10] Miehe, C., Welschinger, F., & Hofacker, M. (2010). Thermodynamically consistent phase-field models of fracture: Variational principles and multi-field FE implementations. International Journal for Numerical Methods in Engineering, 83(10), 1273-1311.
[11] Borden, M. J., Verhoosel, C. V., Scott, M. A., Hughes, T. J., & Landis, C. M. (2012). A phase-field description of dynamic brittle fracture. Computer Methods in Applied Mechanics and Engineering, 217-220, 77-95.
[12] Teichtmeister, S., Kienle, D., Aldakheel, F., & Keip, M. A. (2017). Phase field model for fracture with anisotropic surface energy. Computer Methods in Applied Mechanics and Engineering, 312, 158-172.
[13] Guo, T., & Li, Y. (2022). A phase-field-cohesive zone model for ductile fracture in metal-matrix composites. International Journal of Plasticity, 148, 103141.
[14] Shu W, Stanciulescu I. Fully coupled thermo-mechanical cohesive zone model with thermal softening: Appliaction to nanocomposites[J]. International Journal of Solids and Structures, 2020, 188-189: 1-11.
[15]Huang J, Guo Y, Qin D, et al. Influence of stress triaxiality on the failure behavior of Ti-6Al-4V alloy under a broad range of strain rates[J]. Theoretical and Applied Fracture Mechanics, 2018, 97: 48-61.
[16] Cheng Haixia, Sun Baozhong. Effect of Temperature on Interfacial Properties of Carbon Fiber/Epoxy Composites [J]. Journal of Donghua University (Natural Science Edition), 2016, 42(3): 318-322.
[17] Tan Xueming, Wang Ruifeng, Guo Xiaojun, et al. Study on Failure Characteristics and Failure Model of Superalloy GH4169 [J]. Applied Mathematics and Mechanics, 2021, 42(8): 803-812.